Applied Physics Letters ARTICLE pubs.aip.org/aip/apl

Spin glass and complex magnetism in a high-entropy spinel oxide with five cations at both tetrahedral and octahedral sites

Cite as: Appl. Phys. Lett. **126**, 051901 (2025); doi: 10.1063/5.0242505
Submitted: 4 October 2024 · Accepted: 22 January 2025 ·
Published Online: 3 February 2025

Neha Sharma,[1] J. Link,[2] I. Heinmaa,[2] R. Stern,[2] Tanmoy Chakrabarty,[2,3,a)] and Sourav Marik[1,a)]

AFFILIATIONS

[1]Department of Physics and Material Science, Thapar Institute of Engineering and Technology, Patiala 147004, India
[2]National Institute of Chemical Physics and Biophysics, 12618 Tallinn, Estonia
[3]Division of Sciences, Krea University, Sri City, Andhra Pradesh 517646, India

[a)]**Authors to whom correspondence should be addressed:** tanmoy.chakrabarty@krea.edu.in and soumarik@thapar.edu

ABSTRACT

We report the stabilization and investigation of a hitherto unexplored high-entropy spinel oxide with the composition $(Mg_{0.2}Co_{0.2}Ni_{0.2}Cu_{0.2}Zn_{0.2})(Cr_{0.4}Mn_{0.4}Fe_{0.4}Al_{0.4}Ga_{0.4})O_4$, representing the spinel compound with five distinct elements at both the tetrahedral and octahedral sites in the spinel structure. Detailed structural characterization using x-ray diffraction (and scanning electron microscopy) confirms the cubic crystal structure, while DC magnetic and AC susceptibility measurements reveal complex magnetic behavior below 150 K and spin glass state at 37 K. AC susceptibility measurements along with zero-field-cooled and field-cooled memory effect and aging effect confirm the spin glass state of the material. The power law and Vogel–Fulcher analyses confirm this material's cluster spin glass state. This work highlights the potential of entropy-driven design in tailoring multifunctional materials for advanced applications.

High entropy oxides (HEOs) have recently emerged as a transformative frontier in materials science, with the potential to fundamentally reshape material design and properties.[1,2] HEOs are characterized by significant configurational entropy, resulting from forming a solid solution where multiple metal cations (typically five or more) share a single sublattice. For these oxides, the configurational entropy becomes so dominant that it influences the free energy ($\Delta G = \Delta H - T\Delta S_{mix}$) during high-temperature material synthesis. In this equation, ΔG denotes the change in Gibbs free energy, ΔH is the enthalpy change, and the mixing entropy (ΔS_{mix}) is given by $\Delta S_{mix} = -R\sum x_i \ln(x_i)$. Consequently, the formation of the single-phase solid solution is often governed more by entropy than by enthalpy.[3] The pioneering work by Rost *et al.*[4] in 2015 that stabilized and investigated the high-entropy oxide (HEOs), $(Mg_{0.2}Co_{0.2}Ni_{0.2}Cu_{0.2}Zn_{0.2})O$, marked a significant milestone in the development of HEOs. Since then, HEOs have garnered considerable attention due to their exceptional structural integrity, remarkable multi-functional properties, and enhanced flexibility in the material's design provided by the incorporation of multiple cations within their structure.[1,2,5,6]

The inherent disorder and augmented design flexibility in entropy-stabilized systems significantly enhance their functional properties. Notable examples include high entropy-protected magnetism[7] and tunable magnetism[8] in spinel oxides, sizable magnetic frustration and high exchange bias fields,[9,10] robust ferrimagnetism in spinel thin films,[11] extremely high colossal magnetoresistance in high-entropy manganites,[12] and superior catalytic performance in Al-based spinels.[13] Further, remarkably improved corrosion resistance,[14] extraordinary increase in electrochemical ammonia generation,[15] and promising thermoelectric properties with record-low thermal conductivity[16] are observed in HEOs.

Herein, we present a high entropy spinel oxide with a composition of $(Mg_{0.2}Co_{0.2}Ni_{0.2}Cu_{0.2}Zn_{0.2})(Cr_{0.4}Mn_{0.4}Fe_{0.4}Al_{0.4}Ga_{0.4})O_4$. This is a spinel compound having five different elements in both the A and B sites of the spinel structure (AB_2O_4). In the spinel structure, denoted as AB_2O_4, A cations occupy the tetrahedral sites, while B cations reside in the octahedral sites. The B cations form a pyrochlore-like network, and the A cations establish a diamond-like lattice that exhibits collinear antiferromagnetic order.[17–19] Exploiting this exceptional structure, the high entropy spinel oxides have become a fertile ground for realizing intriguing physicochemical phenomena.[7–11,13,20–23] Further, the high entropy stabilization route provides a powerful approach for fine-tuning materials at the atomic scale, allowing for the development of

materials with tailored properties to meet specific requirements. Therefore, a strong motivation exists to explore interesting strongly correlated high entropy oxides possessing unique structures and fascinating properties. In this paper, we present structural, microstructural, and spin glass properties of a high entropy spinel oxide $(Mg_{0.2}Co_{0.2}Ni_{0.2}Cu_{0.2}Zn_{0.2})(Cr_{0.4}Mn_{0.4}Fe_{0.4}Al_{0.4}Ga_{0.4})O_4$.

The conditions for material synthesis and additional experimental details are provided in the supplementary material. Figure 1(a) presents the Rietveld refinement of the room temperature (RT) x-ray diffraction (XRD) pattern for this material, confirming a cubic crystal structure ($Fd\bar{3}m$) with lattice parameters (a = b = c = 8.3067 (2) Å). Figure 1(c) displays a representative scanning electron microscopy (SEM) image, along with the results of energy-dispersive x-ray spectroscopy (EDS) elemental mapping. It reveals a near stoichiometric composition of the material. The results of the EDS analysis performed on the different positions of the sample are provided in the supplementary material (Table S2). It reveals that all elements are near stoichiometric and uniformly distributed within the sample at the micrometer scale.

Figure 2(a) displays the temperature variation (3–300 K) of the DC magnetization measured at 50 Oe. The temperature-dependent magnetization measurements demonstrate the existence of two peaks, $T_{f1} = 40$ K and $T_{f2} = 75$ K, followed by a large irreversibility in the FC and ZFC magnetization data. Also, the increment in the magnetization data starts below 150 K. Similar to the other spinel materials,[9,10] this significant rise in susceptibility at 150 K strongly suggests a transition to a collinear ferrimagnetic state. Further, the observed peaks (T_{f1} and T_{f2}) in the ZFC magnetization data can be attributed to spin freezing. It is important to note that the high degree of structural disorder likely contributes to this spin-freezing behavior in the sample. In general, transition metal-based spinel oxides (including high entropy oxides) are known for their complex and distinctive magnetic behaviors. For instance, the tetragonal compound $(Mn_{0.2}Co_{0.2}Ni_{0.2}Cu_{0.2}Zn_{0.2})Mn_{1.8}Cr_{0.2}O_4$ exhibits unusual magnetic properties, transitioning from a Néel-type collinear ferrimagnetic order at 85 K to a noncollinear ferrimagnetic order at 23 K.[9,10] $CoMn_2O_4$ showcases two ferrimagnetic orders: a collinear order at 200 K and a non-collinear order at 90 K.[24]

Furthermore, as depicted in the inset of Fig. 2(a), the magnetic susceptibility as a function of temperature was examined under various applied magnetic fields, providing additional insights into the field-dependent magnetic behavior. As the sample is cooled below 150 K, the peaks (T_{f1} and T_{f2}) in the ZFC magnetization shift toward a lower temperature with increasing magnetic field. The magnetic field variation of T_{f1} and T_{f2} is shown in the inset of Fig. 2(b). It is found that T_{f1} follows the non-mean-field scaling theory in the low-field region (below 0.5 T). In non-mean-field scaling theory, $T_f(H) = T_f(0)(1 - AH^{2/\phi})$.[25,26] Here, A represents the amplitude, $T_f(0)$ = freezing temperature in the absence of a magnetic field, and ϕ is the crossover exponent. A value of $\phi = 5.2$ is obtained from the fitting of the T_{f1} values. A similar value of ϕ is observed in the cluster spin glass $Cr_{0.5}Fe_{0.5}Ga$.[26] To further substantiate the complex nature of the material, M-H loops at various temperatures are plotted. The ZFC magnetic field-dependent magnetization measurements (M-H) illustrate a ferrimagnetic-type M-H below T_C [Fig. 2(b)]. However, the opening of

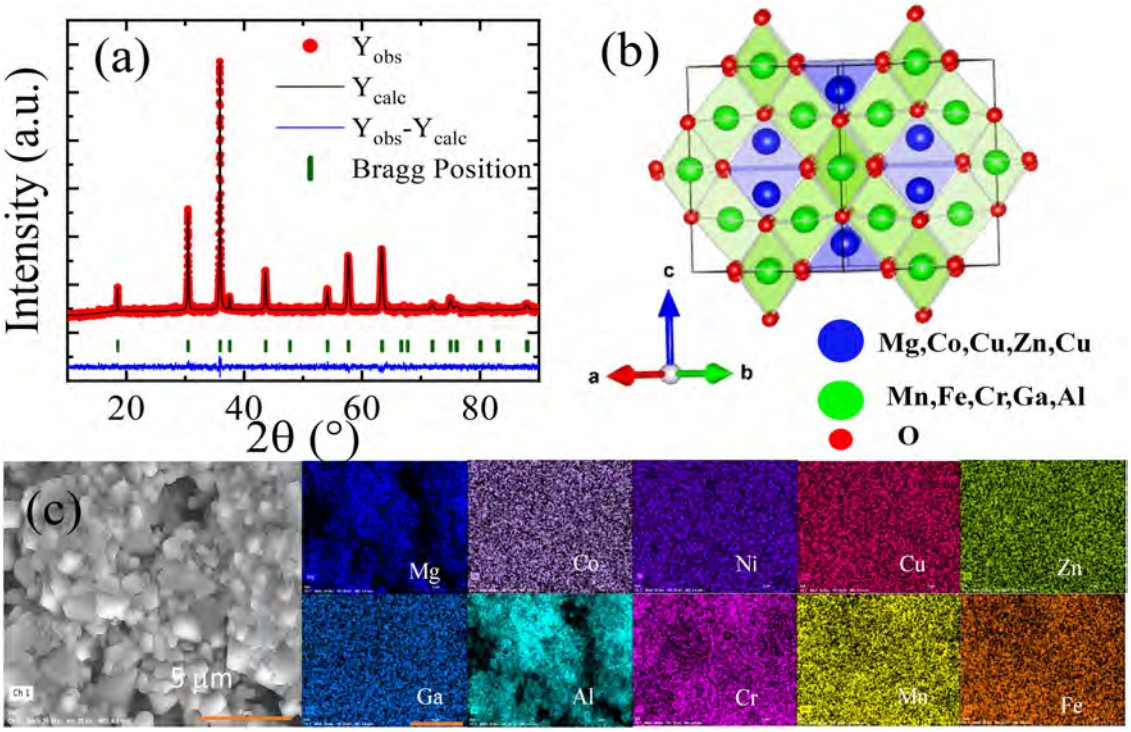

FIG. 1. (a) Rietveld refinement plot of the RT-XRD pattern, (b) crystal structure, and (c) RT FE-SEM image and the EDS mapping of $(Mg_{0.2}Co_{0.2}Ni_{0.2}Cu_{0.2}Zn_{0.2})(Cr_{0.4}Mn_{0.4}Fe_{0.4}Al_{0.4}Ga_{0.4})O_4$.

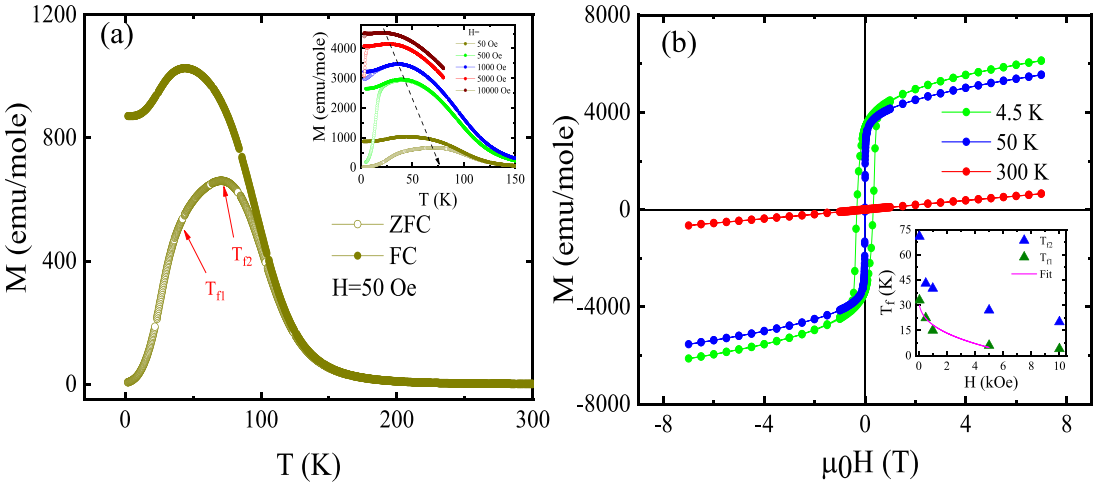

FIG. 2. Temperature dependent (a) FC and ZFC magnetization for $(Mg_{0.2}Co_{0.2}Ni_{0.2}Cu_{0.2}Zn_{0.2})(Cr_{0.4}Mn_{0.4}Fe_{0.4}Al_{0.4}Ga_{0.4})O_4$ measured at 50 Oe. The inset shows the bifurcation between the ZFC and FC susceptibility curves measured in the presence of various magnetic fields. (b) M-H loops at different temperatures. The inset in figure (b) highlights the magnetic field variation of the peak positions in the ZFC magnetization data.

the M-H loop (ferromagnetic type, coercivity) at low temperatures (4.5 K) indicates the possibility of spin glass behavior. Further, the temperature variation of the inverse of the susceptibility (Fig. S1 in the supplementary material) shows a deviation from the linear behavior below 310 K and highlights the possibility of a Griffiths-like phase as observed in several high entropy oxides.[27] The disorder due to the existence of several magnetic cations could originate short-range magnetic correlations above the transition temperature.

In materials exhibiting spin glass behavior, the competing interactions among localized magnetic moments lead to a highly irreversible and metastable state characterized by the absence of long-range magnetic order. This complex state can be effectively analyzed using ac magnetization studies, which provide insights into the dynamic properties of spin glasses. Figure 3(a) presents the temperature dependence of the in-phase component of the ac magnetic susceptibility, $\chi'(T,\nu)$, measured over a temperature range of 16–150 K across a frequency range from 31.6 to 10 000 Hz. Similar to the dc-magnetization, the $\chi'(T,\nu)$ curve reveals a pronounced peak at the freezing temperature, $T_{f2} \approx 80$ K and a smeared peak at $T_{f1} \approx 37$ K. The out-of-phase component of the ac susceptibility, $[\chi''(T,\nu))$, also exhibits peaks near 80 and 37 K. In both $\chi'(T,\nu)$ and $\chi''(T,\nu)$, the peak at 80 K $((T_{f2})]$ shows minimal frequency dependence [Fig. 3(b)]. However, the peak at $T_{f1} \approx 37$ K is much stronger and pronounced in the imaginary component of the ac magnetic susceptibility $\chi''(T,\nu)$ compared to the in-phase component of $\chi'(T,\nu)$. Notably, for $\chi''(T,\nu)$, this peak exhibits frequency dependence, shifting to higher temperatures as the frequency ν increases from 31.6 to 10 000 Hz. This frequency shift of the freezing temperature (T_{f1}) in the imaginary component of ac magnetic susceptibility is the key signature of the spin glass state, reflecting the slowing down of spin dynamics as the system approaches T_{f1}. These peaks shift to higher temperatures with increasing frequency, and their magnitudes are strongly frequency-dependent.

This frequency dispersion of the ac magnetic susceptibility peaks is a well-known characteristic of spin glass systems. It has been

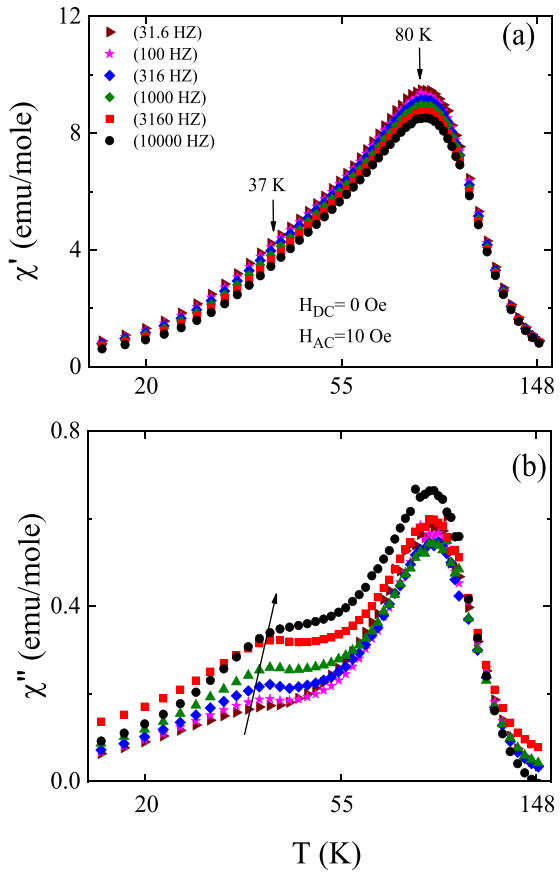

FIG. 3. (a) Temperature dependence of the real part of AC susceptibility $\chi'(T,\nu)$ measured at different frequencies (31.6–10 000 Hz). (b) Temperature dependence of the imaginary component of the ac susceptibility $[\chi''(T,\nu)]$.

observed in various oxide materials with spin glass behavior, including $BiFeO_3$,[28] $CoGaAlO_4$,[29] and $Zn_3V_3O_8$.[30] The observed frequency dependence indicates short-range spin interactions and dynamic slowing down as the system approaches the spin glass state. At higher temperatures, above T_{f2}, $\chi''(T)$ gradually sets to a value nearly zero, while below T_{f1} and T_{f2}, it splits and assumes a non-zero value. This behavior is a characteristic of the spin glass (SG) transition[30,31] and allows us to distinguish the SG compounds from the disordered antiferromagnetic systems.

The spin glass state of the material is further confirmed through memory effect measurements [ZFC and FC, Figs. 4(a) and 4(b)]. To investigate the memory effect in the dc magnetization, we followed a specific protocol to measure the ZFC magnetization.[32] In this protocol, the sample was first cooled down from 150 K in the absence of a magnetic field to 10 K continuously; after reaching 10 K, a weak magnetic field (50 Oe) was applied, and the susceptibility was recorded (continuous measurements) on heating the sample at 1 K/min rate. On reaching 150 K, the magnetic field was turned off. Then, the same procedure to cool the sample is followed (in ZFC mode), but this time, while cooling the sample from 150 to 10 K, we made two pauses at 23 and 15 K, respectively, for 8 h each. In this case, when the magnetization data were recorded while heating the sample from 10 K at the same rate of 1 K/min, we observed dips at those temperatures where we made pauses while cooling. This behavior points to the fact that the system remembers the procedures applied to it. This observance of the memory effect in ZFC measurements confirms the glassiness in our system.[33,34] To investigate the presence of a memory effect in the FC dc magnetization, the magnetization was recorded while cooling the sample from 110 to 10 K at a constant rate of 1 K/min under a 200 Oe magnetic field. During the cooling process, the temperature was paused at 23 and 15 K for a waiting time of 4 h at each pause. During these intervals, the magnetic field was turned off, allowing the system to relax. After each waiting period, the cooling process was resumed. Once the cooling reached 10 K, the sample was reheated continuously under the same magnetic field and heating rate, while recording the magnetization data. The magnetization obtained from this protocol, referred to as M_{FCW}^{Mem}, shows changes in slope at 23 and 15 K, despite no stops occurring at these temperatures during reheating. These (both FC and ZFC) behavior demonstrates that the system retains a "memory" of its prior cooling history, a hallmark feature of spin glasses. For comparison, a reference curve (M_{FCC}^{Ref}) was recorded by continuously cooling the sample under a 200 Oe magnetic field without any interruptions, emphasizing the difference in behavior. We have also observed the aging effect in our system, providing further evidence for the emergence of a spin glass (SG) state in our high-entropy oxide system. To study this effect, the sample was cooled to 20 K in the zero-field-cooled (ZFC) mode, and a magnetic field of 200 Oe was applied after varying waiting times. The magnetization was then recorded as a function of time. Figure 4(c) presents the evolution of magnetization with time in the metastable state. As shown in the figure, the magnetization grows more slowly for longer waiting times, indicating the metastable nature of the low-temperature magnetic state. This behavior is a characteristic of spin glass systems[30] and further supports the presence of a SG state in the sample.

Next, we aim to categorize the spin glass (SG) nature of our high entropy oxide (HEO) system. To quantify the frequency dependence of the spin freezing temperature, we have calculated the Mydosh parameter (S), a commonly used metric for analyzing the relative shift in χ''_{AC} with frequency, as shown in Fig. 4(b). The Mydosh parameter is defined as

$$S = \frac{\Delta T_f}{T_f \Delta \log f},$$

where $(\Delta T_f = T_{f1}(f_1) - T_{f1}(f_2))$ and $\Delta \log_{10} f = \log_{10} f_1 - \log_{10} f_2$, with f_1 and f_2 representing the initial and final frequencies, respectively.[35] Here, T_f indicates the freezing temperature corresponding to T_{f1} in the $(\chi''(T, \nu))$ plot shown in Fig. 3(b). For our HEO material, the Mydosh parameter S is calculated to be approximately 0.053 at around 40 K, which is indicative of glassy behavior. This value of S is significantly larger than that typical of canonical spin glasses such as AuMn ($S \approx 0.0045$),[36] yet it remains below the values commonly observed in superparamagnets, such as holmium borate [α-$(Ho_2O_3(B_2O_3))$] where $S \approx 0.3$.[37] The intermediate value of S suggests that the material exhibits characteristics of a cluster spin glass,

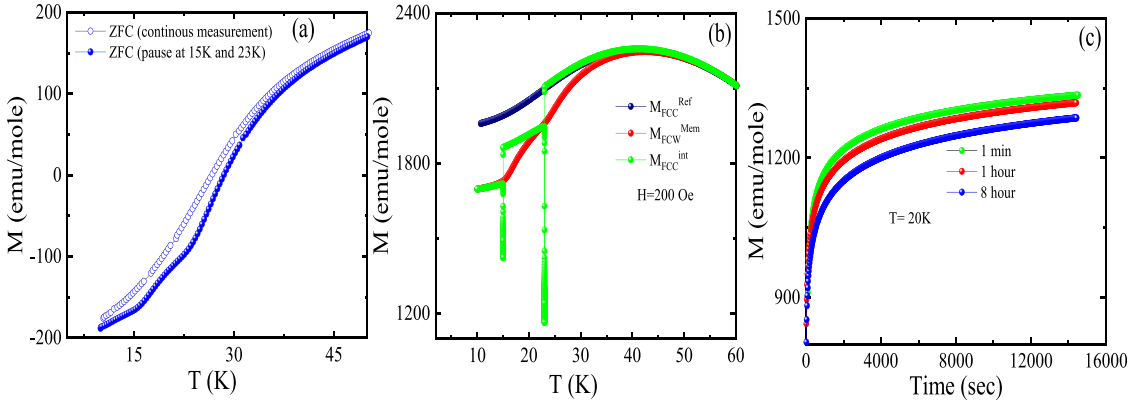

FIG. 4. The memory effect as a function of temperature is studied using the (a) zero-field-cooled (ZFC) and (b) field-cooled (FC) protocol, as described in the text. The observed negative values in the ZFC data are attributed to the trapped field present in the PPMS. (c) The aging effect is evidenced by the growth of magnetization over time. To observe this, the sample was cooled to 20 K in the zero-field-cooled (ZFC) mode, and a magnetic field of 200 Oe was applied after varying time intervals of 1 min, 1, and 8 h.

where spins form short-range correlated clusters rather than displaying long-range magnetic order.[29] Similar values of S have been observed in other cluster spin glass systems, such as ZnV_3O_8 ($S = 0.028$),[30] $NiCr_2O_4$ ($S = 0.016$ and 0.041),[38] and $CoAl_2O_4$($S = 0.037$).[39] The observed intermediate Mydosh parameter in our HEOs suggests a slow relaxation process, potentially signaling a transition to a cluster spin glass phase characterized by short-range interactions. Analyzing the frequency dependence of the AC susceptibility offers valuable insights into the characteristics of the low-temperature glassy phase. A well-established approach involves examining the relaxation time $\tau = \frac{1}{2\pi\nu}$ in relation to the temperature shift of the peak in AC susceptibility, described by the power law,[40]

$$\frac{\tau}{\tau_0} = \left(\frac{T_f}{T_g} - 1\right)^{-z\nu},$$

where τ_0 is the characteristic relaxation time, T_g is the spin glass ordering temperature, T_f is the freezing temperature at a specific observation time, and $z\nu$ is the critical dynamical exponent. This relationship is instrumental in revealing the spin dynamics of magnetic particles near the transition temperature. In our high entropy oxides (HEOs), fitting this power law [Fig. 5(a)] yields parameters $T_g \approx 36$ K, $z\nu = 3.76$, and

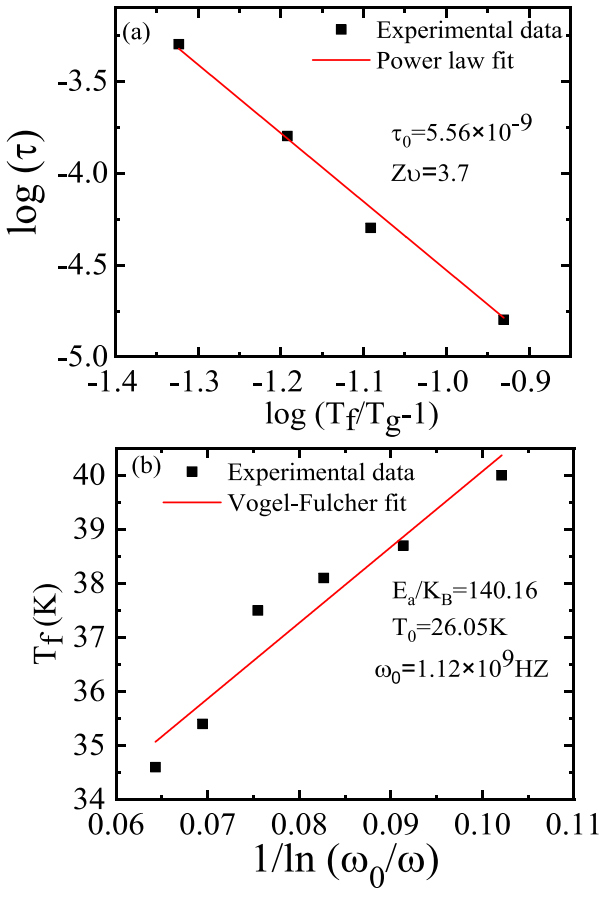

FIG. 5. (a) The best fit of power law and (b) the best fit of Vogel–Fulcher law for $(Ni_{0.2}Mg_{0.2}Co_{0.2}Cu_{0.2}Zn_{0.2})(Mn_{0.4}Fe_{0.4}Cr_{0.4}Ga_{0.4}Al_{0.4})O_4$.

$\tau_0 \approx 5.56 \times 10^{-9}$ s. For conventional spin glass systems, the characteristic relaxation time τ_0 typically lies between 10^{-10} and 10^{-13} s (Refs. 40 and 41) and between 10^{-7} and 10^{-10} s for cluster SG.[26] The significantly larger τ_0 value obtained for our HEOs suggests a deviation from canonical spin glass behavior, pointing instead to the presence of a cluster glass phase characterized by a slower spin dynamics. For instance, a similar value of $z\nu$ value (4.2) and characteristic relaxation time (1.1×10^{-10}) is observed for the cluster SG system $Cr_{0.5}Fe_{0.5}Ga$.[26]

Further, we have analyzed the frequency dependence using the Vogel–Fulcher (VF) law[42] and determined the activation energy of the relaxation process in the glassy phase. The VF law is given by

$$\omega = \omega_0 \exp\left(-\frac{E_a}{k_B(T_f - T_0)}\right),$$

where ω_0 = characteristic frequency, ω = angular frequency ($\omega = 2\pi\nu$), E_a = activation energy, T_0 = Vogel–Fulcher temperature, and k_B = Boltzmann constant. The best fit to the VF law, shown in Fig. 5(b), is obtained with parameters $\omega_0 = 1.12 \times 10^9$ Hz, $E_a/k_B = 140$ K, and $T_0 = 26.05$ K.

The characteristic frequency ω_0 obtained from the fitting is significantly lower than that typically found in conventional spin glass systems, which is around 10^{13} s.[43] This lower ω_0 value is indicative of slower dynamics, which aligns with the behavior expected in a cluster glass rather than a canonical spin glass. Additionally, the values of E_a/k_B and T_0 are both positive and in the range of tens of Kelvin, which is consistent with the cluster glass behavior observed in similar systems.[44]

In this study, we have stabilized and comprehensively investigated a previously unexplored high entropy spinel compound having five different elements in both the A and B sites of the spinel structure (AB_2O_4). Through comprehensive structural and microstructural characterizations, as well as detailed dc and ac magnetic measurements, we demonstrated that $(Mg_{0.2}Co_{0.2}Ni_{0.2}Cu_{0.2}Zn_{0.2})(Cr_{0.4}Mn_{0.4}Fe_{0.4}Al_{0.4}Ga_{0.4})O_4$ exhibits a complex magnetic behavior below 150 K and a spin glass state below 37 K. Our detailed AC susceptibility measurements along with the ZFC and FC memory effect, and aging effect provide critical insights into the magnetic behavior, confirming the spin glass nature of this high entropy oxide. Furthermore, the Vogel–Fulcher analysis and dynamic scaling investigations reveal critical exponents consistent with cluster spin glass characteristics. This research highlights the potential of incorporating a diverse range of elemental constituents into the crystallographic sites of complex spinel oxide frameworks. It also emphasizes the promising opportunities for tailoring and enhancing magnetic properties in strongly correlated systems, paving the way for innovative applications in this class of materials.

See the supplementary material for the detailed experimental section, structural parameters obtained from the Rietveld refinements, EDS details, and the temperature-dependent inverse of the susceptibility.

S.M. acknowledges the ANRF (formerly SERB), Government of India, for the (SRG/2021/001993) Start-up Research Grant. Work in Tallinn was supported by the European Regional Development Fund (Awards TK133 and TK134) and the Estonian Research Council (Projects Nos. PRG4 and PRG1702). This study was co-funded by the European Union and Ministry of Education and Research via Project No. TEM-TA25.

AUTHOR DECLARATIONS

Conflict of Interest

The authors have no conflicts to disclose.

Author Contributions

Neha Sharma: Data curation (equal); Formal analysis (lead); Investigation (lead); Methodology (equal); Validation (equal); Writing – original draft (lead). **Joosep Link:** Data curation (equal); Investigation (equal); Writing – review & editing (supporting). **Ivo Heinmaa:** Data curation (equal); Investigation (equal); Writing – review & editing (supporting). **Raivo Stern:** Investigation (equal); Resources (equal); Writing – review & editing (equal). **Tanmoy Chakrabarty:** Conceptualization (equal); Data curation (equal); Investigation (equal); Writing – review & editing (equal). **Sourav Marik:** Conceptualization (lead); Funding acquisition (lead); Project administration (lead); Supervision (lead); Writing – review & editing (equal).

DATA AVAILABILITY

The data that support the findings of this study are available from the corresponding author upon reasonable request.

REFERENCES

[1]W.-E. Ke, J.-W. Chen, C.-E. Liu, Y.-C. Ku, C.-F. Chang, P. Shafer, S.-J. Lin, M.-W. Chu, Y.-C. Chen, J.-W. Yeh *et al.*, Adv. Funct. Mater. **34**, 2312856 (2024).
[2]S. S. Aamlid, M. Oudah, J. Rottler, and A. M. Hallas, J. Am. Chem. Soc. **145**, 5991 (2023).
[3]C. Oses, C. Toher, and S. Curtarolo, Nat. Rev. Mater. **5**, 295 (2020).
[4]C. M. Rost, E. Sachet, T. Borman, A. Moballegh, E. C. Dickey, D. Hou, J. L. Jones, S. Curtarolo, and J.-P. Maria, Nat. Commun. **6**, 8485 (2015).
[5]Y. Jiao, J. Dai, Z. Fan, J. Cheng, G. Zheng, L. Grema, J. Zhong, H.-F. Li, and D. Wang, Mater. Today **77**, 92 (2024).
[6]W. Xu, E. Diesen, T. He, K. Reuter, and J. T. Margraf, J. Am. Chem. Soc. **146**, 7698 (2024).
[7]L. Min, J. P. Barber, Y. Wang, S. V. Gayathri Ayyagari, G. E. Niculescu, E. Krysko, G. R. Bejger, L. Miao, S. H. Lee, Q. Zhang, N. Alem, C. M. Rost, and Z. Mao, J. Am. Chem. Soc. **146**, 24320 (2024).
[8]B. Musicó, Q. Wright, T. Z. Ward, A. Grutter, E. Arenholz, D. Gilbert, D. Mandrus, and V. Keppens, Phys. Rev. Mater. **3**, 104416 (2019).
[9]N. Sharma, S. Jangid, S. Choudhury, S. K. Mahatha, R. P. Singh, and S. Marik, Appl. Phys. Lett. **123**, 161901 (2023).
[10]N. Sharma, S. Mandal, S. Choudhury, S. K. Mahatha, and S. Marik, Scr. Mater. **244**, 116017 (2024).
[11]F. Jin, Y. Zhu, L. Li, Z. Pan, D. Pan, M. Gu, Q. Li, L. Chen, and H. Wang, Adv. Funct. Mater. **33**, 2214273 (2023).
[12]A. Sarkar, D. Wang, M. V. Kante, L. Eiselt, V. Trouillet, G. Iankevich, Z. Zhao, S. S. Bhattacharya, H. Hahn, and R. Kruk, Adv. Mater. **35**, 2207436 (2023).
[13]R. R. Katzbaer, F. M. dos Santos Vieira, I. Dabo, Z. Mao, and R. E. Schaak, J. Am. Chem. Soc. **145**, 6753 (2023).
[14]N.-L. Chen, G.-T. Sun, C.-Y. He, B.-H. Liu, H.-X. Feng, G. Liu, and X.-H. Gao, Mater. Today Phys. **42**, 101363 (2024).
[15]S. Sun, P. Z. Chencheng Dai, S. Xi, Y. Ren, H. R. Tan, P. C. Lim, C. D. Ming Lin, D. Zhang, A. Y. Chao Wu, J. C. J. Koh, W. Y. Lieu, D. H. L. Seng, L. Sun, Y. Li, T. L. Tan, J. Zhang, Z. J. Xu, and Z. W. Seh, Nat. Commun. **15**, 260 (2024).
[16]S. S. Jana and T. Maiti, Mater. Horiz. **10**, 1848 (2023).
[17]X. Wang, B. L. Musicó, C. Kons, P. C. Metz, V. Keppens, D. A. Gilbert, Y. Zhang, and K. Page, APL Mater. **10**, 2102157 (2022).
[18]N. Büttgen, J. Hemberger, V. Fritsch, A. Krimmel, M. Mücksch, H. K. von Nidda, P. Lunkenheimer, R. Fichtl, V. Tsurkan, and A. Loidl, New J. Phys. **6**, 191 (2004).
[19]P. Mohanty, N. Sharma, D. Singh, Y. Breard, D. Pelloquin, S. Marik, and R. Singh, Phys. Rev. Mater. **7**, 084408 (2023).
[20]H. Jiang, K. Yu, X. Liu, L. He, B. He, and M. Huang, Scr. Mater. **237**, 115683 (2023).
[21]R. Das, D. Ghosh, S. Bhattacharya, S. Chowdhury, V. M. A. P. Singh, S. Ghosh, A. Gayen, and M. M. Seikh, J. Phys. Chem. C **128**, 14168 (2024).
[22]N. Sharma, S. Mandal, and S. Marik, *Structure, Raman spectroscopy, and magnetic properties of new Al, Ga, and Mn-based high entropy oxides Ceramics International* (Ceramics International, 2024), Vol. 50, pp. 48200–48209.
[23]N. Sharma, N. Sharma, J. Sharma, S. D. Kaushik, S. K. Mahatha, T. Chakraborty, and S. Marik, Phys. Rev. B **110**, 224432 (2024).
[24]B. Poojitha, A. Shaji, S. Badola, and S. Saha, J. Chem. Phys. **156**, 184701 (2022).
[25]A. P. Malozemoff, S. E. Barnes, and B. Barbara, Phys. Rev. Lett. **51**, 1704 (1983).
[26]P. Bag, P. R. Baral, and R. Nath, Phys. Rev. B **98**, 144436 (2018).
[27]R. Das, S. Sen, S. Chowdhury, S. Bhattacharya, S. Mondal, T. K. Mandal, A. Gayen, V. Mutta, and M. M. Seikh, J. Phys. Chem. C **129**(1), 940–953 (2025).
[28]S. Nakamura, S. Soeya, N. Ikeda, and M. Tanaka, J. Appl. Phys. **74**, 5652 (1993).
[29]T. J. Bullard, M. A. Susner, K. M. Taddei, J. Brant, and T. Haugan, Sci. Rep. **11**, 11355 (2021).
[30]T. Chakrabarty, A. V. Mahajan, and S. Kundu, J. Phys. Condens. Matter **26**, 405601 (2014).
[31]S. Süllow, G. J. Nieuwenhuys, A. A. Menovsky, J. A. Mydosh, S. A. M. Mentink, T. E. Mason, and W. J. L. Buyers, Phys. Rev. Lett. **78**, 354 (1997).
[32]P. Nordblad, Phys. Scr. **88**, 058301 (2013).
[33]V. Dupuis, E. Vincent, J. Hammann, J. E. Greedan, and A. S. Wills, J. Appl. Phys. **91**, 8384 (2002).
[34]M. Sasaki, P. E. Jönsson, H. Takayama, and H. Mamiya, Phys. Rev. B **71**, 104405 (2005).
[35]J. Mydosh, J. Magn. Magn. Mater. **157–158**, 606 (1996).
[36]C. A. M. Mulder, A. J. van Duyneveldt, and J. A. Mydosh, Phys. Rev. B **25**, 515 (1982).
[37]J. A. Mydosh, *Spin Glasses: An Experimental Introduction* (Taylor and Francis, London, 1993).
[38]A. M. Nashaat, M. A. Kassem, A. A. El-Fadl, and H. Nakamura, Nanotechnology **35**, 195702 (2024).
[39]K. Hanashima, Y. Kodama, D. Akahoshi, C. Kanadani, and T. Saito, J. Phys. Soc. Jpn. **82**, 024702 (2013).
[40]D. Nam, R. Mathieu, P. Nordblad, N. Khiem, and N. Phuc, Phys. Rev. B **62**, 8989 (2000).
[41]B. Maji, K. G. Suresh, and A. K. Nigam, J. Phys. Condens. Matter **23**, 506002 (2011).
[42]S. Shtrikman and E. Wohlfarth, Phys. Lett. A **85**, 467 (1981).
[43]S. Banerjee, D. P. Panda, P. Yanda, and A. Sundaresan, Phys. Rev. Mater. **7**, 034405 (2023).
[44]S. Nayak, S. Ghorai, A. M. Padhan, S. Hajra, P. Svedlindh, and P. Murugavel, Phys. Rev. B **106**, 174402 (2022).